Which Multi-Core Fiber Layout is Best for Highest Capacity Network Design?

Yuya Seki(1), Yosuke Tanigawa(1), Yusuke Hirota(2), Hideki Tode(1)

(1) Graduate School of Informatics, Osaka Metropolitan University, Japan, tode@omu.ac.jp
(2) National Institute of Information and Communications Technology, Japan

Abstract *We investigate core pitch dependence of the power coupling coefficient and which multi-core fiber (MCF) layout is best for achieving the highest capacity. We demonstrate that 22-core MCFs with 7-concentric circular structures can accommodate approximately 175% higher traffic loads than irregular hexagonal 27-core MCFs.*

Introduction

To achieve the largest transmission capacity in space-division multiplexing elastic optical networks[1]–[3] for given network topologies, data transfer routes, and modulation formats, a lightpath must be efficiently established so that intercore crosstalk (IC-XT) in multi-core fibers (MCFs) along the path is within the tolerance threshold. Many researchers engaged in reducing IC-XT in MCF environments[2]–[4]. The IC-XT can be decreased by optimizing the core arrangement or refractive index profile when fabricating fibers[5]–[13] or avoiding using adjoining cores in resource allocation[14]. However, the former does not consider the lightpath length and modulation format level; the latter only discusses hexagonal MCFs. A recent study showed trench-assisted heterogeneous MCFs are optimal to accommodate more lightpaths[15]. However, they also only consider hexagonal MCFs and require a large core pitch for IC-XT suppression despite that an upper limit must be set to the core pitch for acceptable failure probability and bending loss[12],[16]–[18].

To our best knowledge, no study discusses how densely the cores can be packed within tolerant IC-XT based on the upper limit of the core pitch, network topology, routing, and modulation format selection method. The number of adjacent cores, core pitch, and path length all affect the IC-XT amount, and the IC-XT tolerance threshold depends on the assigned modulation format. Therefore, we need to consider them in a unified manner to improve spatial density.

This paper discusses how to place cores densely within tolerant IC-XT with fixed cladding diameters efficiently for candidate paths and modulation formats. The contributions are: i) provide a simple estimation of power coupling coefficients for weakly coupled MCFs with different core pitches; ii) explain the crosstalk-free (XT-free) concept as a condition in which the IC-XT effect is eliminated in the core and spectrum assignment based on previous work; iii) compare the simulated blocking probabilities for various MCF core placements and demonstrate that XT-free condition is essential for increasing the network capacity effectively.

Core Pitch Dependence of Crosstalk

In MCF optical networks, the adverse effect of IC-XT must be considered. We can estimate the amount of IC-XT of weakly-coupled MCFs $XT(L;n)$ by the following formula[3]–[5],[15]:

$$XT(L;n) = \frac{n\left[1-\exp\left\{-(n+1)hL\right\}\right]}{1+n\exp\left\{-(n+1)hL\right\}}, \qquad (1)$$

where h, n, and L are the power coupling coefficient, number of neighbor lit-cores, and propagation distance, respectively. Power coupling coefficient is calculated by $h = \frac{2\kappa^2(\Lambda)R}{\beta\Lambda}$[3],[5],[7],[8],[15], where Λ, $\kappa(\Lambda)$, R, and β are the core pitch, mode coupling coefficient as a function of core pitch, bending radius, and propagation constant, respectively. Note that we focus on single-mode homogeneous MCFs in this paper. The mode coupling coefficient is described with the approximation derived by Hankel's expansion[8],[19]: $\kappa(\Lambda) = C\sqrt{\frac{\pi a}{2W\Lambda}}\exp\left(-\frac{W}{a}\Lambda\right)$, where C, W, and a are Λ-independent factor, the normalized transverse wave number in the cladding, and core radius, respectively. Hence, we can obtain the core pitch dependence of the power coupling coefficient by

$$\Delta h_{\text{dB}} \overset{def}{=} \frac{\partial}{\partial\Lambda}\left\{10\log_{10}(hL)\right\} = -10\left(\frac{2W}{a}+\frac{2}{\Lambda}\right)\log_{10} e. \qquad (2)$$

According to Kumar et al.[8], W is expressed by $W = ak\sqrt{n_{\text{eff}}^2 - n_0^2}$, where k, n_{eff}, n_0 are the wave number, mode effective refractive index, refractive index of the cladding, respectively. Substituting $n_{\text{eff}} = 1.452\,656$ and $n_0 = 1.45$ yields $\Delta h_{\text{dB}} \approx -3.3\,\text{dB}\,\mu\text{m}^{-1}$ for transmission in C-band where Λ is $30\,\mu\text{m}$ to $60\,\mu\text{m}$. This relationship can be universally applicable to various core arrangements; besides hexagonal MCFs[5],[8],[13], to precisely calculate the difference in power coupling coefficients between nearest-neighbor and diagonal cores of square lattice structure (SLS) MCFs[6]. Although C is a function of Λ in trench-assisted MCFs[12],[15], Eq. (2) still holds because $\frac{\partial \log C}{\partial \Lambda}$ is negligible. In addition, we assume $h = 7.7 \times 10^{-8}\,\text{m}^{-1}$, where $\Lambda = 35.4\,\mu\text{m}$[4]. Therefore, relationship between the power coupling coefficient h (m^{-1}) and core pitch Λ (μm) is:

$$h(\Lambda) = 7.7 \times 10^{-8} \times 10^{\{-0.33\times(\Lambda-35.4)\}}\ \text{m}^{-1}. \quad (3)$$

Core Arrangements and Core Pitch Limitation

We discuss 13 MCF layouts with 10 to 27 cores. These include the 10-, 12-, 14-, and 27-core irregular hexagonal MCFs shown in Tab. 1[7]–[11]; the 12-, 16-, 21-, and 24-core SLS MCFs shown in Tab. 2[10],[12],[13]; the 16-, 19-, 22-, and 25-core k-concentric circle structure (k-CCS) MCFs shown in Tab. 3; and the well-known hexagonal 19-core MCF[3],[7],[8],[10],[12]–[16],[20]. The k-CCS MCFs have cores arranged in concentric circles, with multiples of k on each circumference. This paper considers three-layer k-CCS MCFs. Although there is an option to shift the phase of the outermost ring[16],[21],[22], the phase of each ring is aligned in this paper to minimize the number of neighbor cores. The radii of the inner rings are set to $42.5\,\mu\text{m}$ for the 5- and 6-CCS MCFs, $43.59\,\mu\text{m}$ for the 7-CCS MCF, and $43.33\,\mu\text{m}$ for the 8-CCS MCF. In the cross-sectional figures of the k-CCS MCFs in Tab. 3, the nearest neighbor cores are connected with lines.

The core pitch Λ is calculated from the upper and lower limits of the cladding diameter and thickness, respectively. These limitations exist for acceptable failure rates and bending losses. In this paper, we set the upper limit of cladding diameter to $230\,\mu\text{m}$ and the lower limit of outermost cladding thickness to $30\,\mu\text{m}$[12],[16]–[18]. Tables 1, 2, and 3 show the upper limits of the core pitch Λ under these assumptions.

We define "XT-free" as an environment where IC-XT does not exceed the tolerance threshold even when using all cores. The IC-XT should be considered only between nearest neighbor cores, according to Eq. (3). If the "allowable adjacency" (n_a) of a lightpath shown in Eq. (4) is greater than or equal to the maximum number of neighbor cores, we can assume it to be XT-free[20]:

$$n_a = \left\lfloor \frac{XT_{th}}{h(\Lambda)\sum_{l\in l_p} L(l)} \right\rfloor, \quad (4)$$

where XT_{th}, l_p, and $L(l)$ are the tolerance threshold of IC-XT, the set of links that constitute the lightpath, and the length of link l, respectively. Note that the value of the allowable adjacency indicator depends on the routing and modulation format assignment methods.

Experimental Results

We prepared an evaluation scenario on the TMN12 topology[23]. One MCF was set on each link in each transmission direction and had 320 frequency slots for each core. Each lightpath establishment request arrives for each source and destination pair with the average rate that is changed as a parameter and the average holding time of $5\,\text{s}$. Both the arrival interval and holding time follow exponential distributions. Each lightpath was allocated the shortest path and the highest level modulation format as long as the route distance does not exceed its transmission reach[20]. Five modulation formats, i.e., BPSK, QPSK, 8-QAM, 16-QAM, and 32-QAM, were supported, with transmission distances of 6300, 3500, 1200, 600, and $300\,\text{km}$, required number of fre-

Tab. 1: Irregular Hexagonal Multi-Core Fibers (Prioritized cores are colored orange.)

# of Cores Core Pitch	10 56.67 µm	12[7]–[10] 55.65 µm	14[11] 47.15 µm	27[7],[10] 33.78 µm
TMN12	XT free	XT free	XT free	—
MCF Layout	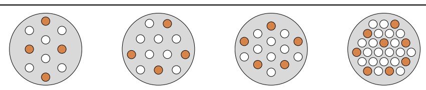			

Tab. 2: Square Lattice Structure Multi-Core Fibers (Prioritized cores are colored orange.)

# of Cores Core Pitch	12[10],[12] 53.76 µm	16[10] 40.07 µm	21[10],[13] 38.01 µm	24[10],[12] 33.34 µm
TMN12	XT free	XT free	XT free	—
MCF Layout	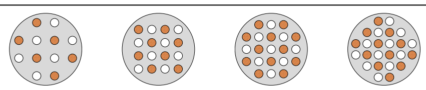			

Tab. 3: k-Concentric Circle Structure Multi-Core Fibers (Prioritized cores are colored orange.)

# of Cores Core Pitch	16 ($k=5$) 42.5 µm	19 ($k=6$) 42.5 µm	22 ($k=7$) 37.83 µm	25 ($k=8$) 33.17 µm
TMN12	XT free	XT free	XT free	—
MCF Layout	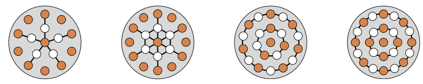			

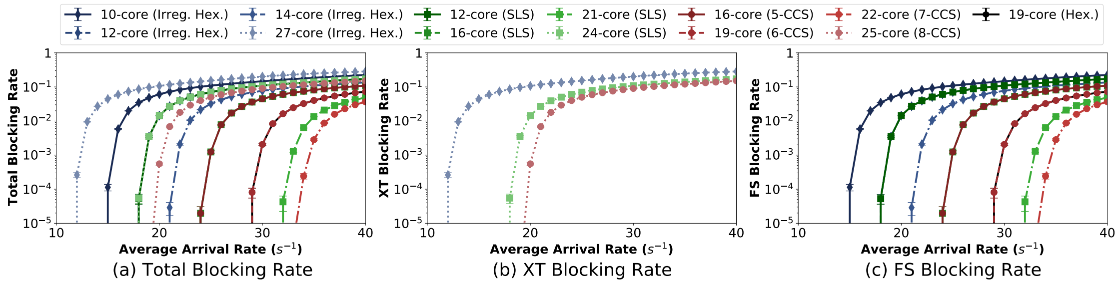

(a) Total Blocking Rate (b) XT Blocking Rate (c) FS Blocking Rate

Fig. 1: Blocking rate properties of the CoreMap method for TMN12 topology

quency slots of 8, 4, 3, 2, and 2 assuming to provide a constant data rate for each connection, and IC-XT tolerance thresholds of -14, -18.5, -21, -25, and $-27\,\mathrm{dB}$, respectively[24]. Core and spectrum were allocated to each lightpath by the CoreMap method[14],[20] that searches available slots preferentially from cores that are not adjacent to each other (prioritized cores)[12],[14] and terminates the search once a feasible solution is found. Here, spectral contiguity and continuity constraints[1],[24] and the implementation of core switches were assumed. Tables 1, 2, and 3 show whether the MCFs are XT-free or not in this experimental environment. The hexagonal 19-core MCF is XT-free from the core pitch of $42.5\,\mu\mathrm{m}$.

The performance indicators are the blocking rate, called “Total Blocking Rate” and its breakdown: “XT Blocking Rate” as the blocking rate due to IC-XT exceeding the tolerance threshold, and “FS Blocking Rate” as the blocking rate due to the lack of available frequency slots.

The results of the blocking rates are shown in Fig. 1, and demonstrate that XT-free MCFs can accommodate more traffic loads than non-XT-free MCFs even when the former MCFs have fewer cores. For example, XT-free 7-CCS 22-core MCF achieves a much lower total blocking rate than non-XT-free 27-core irregular hexagonal MCF, and can accommodate approximately 175% higher traffic loads. This is because only non-XT-free MCFs cause the XT blocking that is more serious compared with the FS blocking in XT-free MCFs. Therefore, even when non-XT-free MCFs are superior in the number of cores, the negative impact of IC-XT tends to decrease the substantial capacity and increases the total blocking rate compared to XT-free MCFs. Among XT-free MCFs, the 7-CCS 22-core MCF achieves the smallest blocking rate in this scenario. Including additional experimental results omitted for reasons of space limitation (JPN12 topology[23]), we can conclude that the XT-free MCFs with the most cores are generally the most effective.

Some other insights are also obtained. The total blocking probabilities of the 12-core SLS-MCF and 24-core SLS MCF are similar. This is because only 12 prioritized cores can be used in the 24-core SLS MCF environment due to the adverse effect of IC-XT. In addition, hexagonal 19-core MCF and 6-CCS 19-core MCF have almost the same total blocking rate (the graphs completely overlapped) because they both are XT-free and have the same core pitch and the number of cores. However, the number of IC-XT sources, i.e., nearest neighbor cores, differs. Hence, for the 19-core MCF, the hexagonal MCF should be replaced by the 6-CCS MCF to prevent the blocking rate caused by IC-XT.

Conclusions and Discussions

In this paper, we discussed what kind of MCF core placement reduces the blocking rate of lightpath establishment requests the most for given network topologies, routes, and modulation formats. We formulated the power coupling coefficient as the function of the core pitch and introduced the XT-free concept. Simulation results show that 7-CCS 22-core MCFs can accommodate approximately 175% higher traffic loads than irregular hexagonal 27-core MCFs in TMN12 topology.

In non-XT-free environments where the effect of IC-XT is not negligible, the blocking rate is higher than that in XT-free MCFs with fewer cores, even providing more ones. For XT-free MCFs, we confirmed that the core search order does not affect the blocking rate through additional experiments. By optimizing the MCF core arrangement and creating XT-free environments, we need not consider IC-XT in the core and spectrum allocation. Thus, we can concentrate on other issues, e.g., defragmentation. Note that whether or not the network environment is XT-free depends on route and modulation format selection discipline because the value of the allowable adjacency indicator varies.

Acknowledgements

This work was supported by JSPS KAKENHI Grant Number 21H04878.

References

[1] B. C. Chatterjee, N. Sarma, and E. Oki, "Routing and spectrum allocation in elastic optical networks: A tutorial", *IEEE Communications Surveys & Tutorials*, vol. 17, no. 3, pp. 1776–1800, 2015. DOI: 10.1109/COMST.2015.2431731.

[2] B. J. Puttnam, G. Rademacher, and R. S. Luís, "Space-division multiplexing for optical fiber communications", *Optica*, vol. 8, no. 9, pp. 1186–1203, 2021. DOI: 10.1364/OPTICA.427631.

[3] G. M. Saridis, D. Alexandropoulos, G. Zervas, and D. Simeonidou, "Survey and evaluation of space division multiplexing: From technologies to optical networks", *IEEE Communications Surveys & Tutorials*, vol. 17, no. 4, pp. 2136–2156, 2015. DOI: 10.1109/COMST.2015.2466458.

[4] K. Takenaga, Y. Arakawa, S. Tanigawa, *et al.*, "An investigation on crosstalk in multi-core fibers by introducing random fluctuation along longitudinal direction", *IEICE Transactions on Communications*, vol. E94-B, no. 2, pp. 409–416, 2011. DOI: 10.1587/transcom.E94.B.409.

[5] T. Hayashi, T. Taru, O. Shimakawa, T. Sasaki, and E. Sasaoka, "Design and fabrication of ultra-low crosstalk and low-loss multi-core fiber", *Optics Express*, vol. 19, no. 17, pp. 16 576–16 592, 2011. DOI: 10.1364/OE.19.016576.

[6] M. Koshiba, Y. Kokubun, M. Nakagawa, M. Ohzeki, and K. Takenaga, "Behavior of intercore crosstalk in square-layout uncoupled four-core fibers", *IEICE Electronics Express*, vol. 19, no. 18, pages 20220379, 2022. DOI: 10.1587/elex.19.20220379.

[7] K. Saitoh, "Multi-core fiber technology for sdm: Coupling mechanisms and design", *Journal of Lightwave Technology*, vol. 40, no. 5, pp. 1527–1543, 2022. DOI: 10.1109/JLT.2022.3145052.

[8] D. Kumar and R. Ranjan, "Estimation of crosstalk in homogeneous multicore fiber for high core count under limited cladding diameter", in *Conference on Information and Communication Technology*, 2017, pp. 1–4. DOI: 10.1109/INFOCOMTECH.2017.8340626.

[9] T. Sakamoto, K. Saitoh, S. Saitoh, *et al.*, "Spatial density and splicing characteristic optimized few-mode multi-core fiber", *Journal of Lightwave Technology*, vol. 38, no. 16, pp. 4490–4496, 2020. DOI: 10.1109/JLT.2020.2987351.

[10] Y. Tobita, T. Fujisawa, T. Sakamoto, *et al.*, "Optimal design of 4LP-mode multicore fibers for high spatial multiplicity", *Optics Express*, vol. 25, no. 5, pp. 5697–5709, 2017. DOI: 10.1364/OE.25.005697.

[11] D. Qian, E. Ip, M.-F. Huang, *et al.*, "1.05 Pb/s transmission with 109 b/s/Hz spectral efficiency using hybrid single- and few-mode cores", in *Frontiers in Optics*, 2012, paper FW6C.3. DOI: 10.1364/FIO.2012.FW6C.3.

[12] F. Ye, K. Saitoh, H. Takara, R. Asif, and T. Morioka, "High-count multi-core fibers for space-division multiplexing with propagation-direction interleaving", in *Optical Fiber Communication Conference*, 2015, paper Th4C.3. DOI: 10.1364/OFC.2015.Th4C.3.

[13] T. Sakamoto, T. Matsui, K. Saitoh, *et al.*, "Low-loss and low-DMD 6-mode 19-core fiber with cladding diameter of less than 250 µm", *Journal of Lightwave Technology*, vol. 35, no. 3, pp. 443–449, 2017. DOI: 10.1109/JLT.2016.2610479.

[14] S. Fujii, Y. Hirota, H. Tode, and K. Murakami, "On-demand spectrum and core allocation for reducing crosstalk in multicore fibers in elastic optical networks", *Journal of Optical Communications and Networking*, vol. 6, no. 12, pp. 1059–1071, 2014. DOI: 10.1364/JOCN.6.001059.

[15] A. Agrawal and S. G. Kulkarni, "Spectrum-efficiency analysis for trench-assisted and heterogeneous-index multicore fiber networks", in *IEEE International Conference on Communications*, 2022, pp. 3022–3027. DOI: 10.1109/ICC45855.2022.9838965.

[16] Y. Goto, K. Nakajima, T. Matsui, T. Kurashima, and F. Yamamoto, "Influence of cladding thickness on transmission loss and its relationship with multicore fiber structure", *Journal of Lightwave Technology*, vol. 33, no. 23, pp. 4942–4949, 2015. DOI: 10.1109/JLT.2015.2493372.

[17] K. Takenaga, Y. Arakawa, Y. Sasaki, *et al.*, "A large effective area multi-core fiber with an optimized cladding thickness", *Optics Express*, vol. 19, no. 26, B543–B550, 2011. DOI: 10.1364/OE.19.00B543.

[18] R. S. Luís, G. Rademacher, B. J. Puttnam, *et al.*, "1.2 Pb/s transmission over a 160 µm cladding, 4-core, 3-mode fiber, using 368 C+L band PDM-256-QAM channels", in *European Conference on Optical Communication*, 2018, pp. 1–3. DOI: 10.1109/ECOC.2018.8535233.

[19] A. Snyder, "Asymptotic expressions for eigenfunctions and eigenvalues of a dielectric or optical waveguide", *IEEE Transactions on Microwave Theory and Techniques*, vol. 17, no. 12, pp. 1130–1138, 1969. DOI: 10.1109/TMTT.1969.1127112.

[20] Y. Seki, Y. Tanigawa, Y. Hirota, and H. Tode, "Core and spectrum allocation to achieve graceful degradation of inter-core crosstalk with generalized hierarchical core prioritization on space-division multiplexing elastic optical networks", *Journal of Optical Communications and Networking*, vol. 15, no. 1, pp. 43–56, 2023. DOI: 10.1364/JOCN.472418.

[21] J. Sakaguchi, W. Klaus, B. J. Puttnam, *et al.*, "19-core MCF transmission system using EDFA with shared core pumping coupled via free-space optics", *Optics Express*, vol. 22, no. 1, pp. 90–95, 2014. DOI: 10.1364/OE.22.000090.

[22] B. J. Puttnam, R. S. Luís, W. Klaus, *et al.*, "2.15 Pb/s transmission using a 22 core homogeneous single-mode multi-core fiber and wideband optical comb", in *European Conference on Optical Communication*, 2015, pp. 1–3. DOI: 10.1109/ECOC.2015.7341685.

[23] *JPN Model*, https://www.ieice.org/cs/pn/eng/jpnm_en.html. (visited on 04/07/2023).

[24] E. E. Moghaddam, H. Beyranvand, and J. A. Salehi, "Crosstalk-aware resource allocation in survivable space-division-multiplexed elastic optical networks supporting hybrid dedicated and shared path protection", *Journal of Lightwave Technology*, vol. 38, no. 6, pp. 1095–1102, 2020. DOI: 10.1109/JLT.2019.2954177.